iScience

CellPress
OPEN ACCESS

Article

A LY6E-PHB1-TRIM21 assembly degrades CD14 protein to mitigate LPS-induced inflammatory response

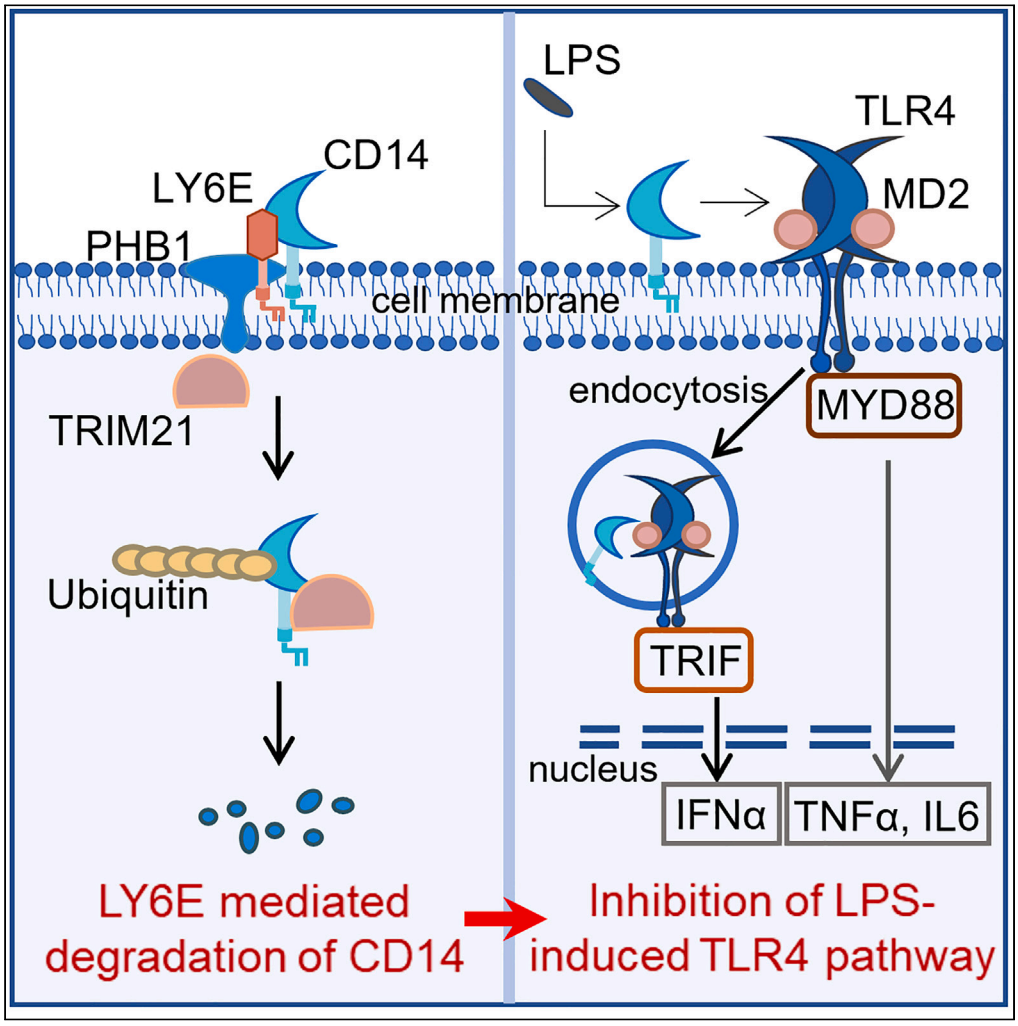

Xinyu Zhu, Linxia Zhang, Daobin Feng, ..., Chen Zhao, Xiaoyan Zhang, Jianqing Xu

chen_zhao72@163.com (C.Z.)
zhangxiaoyan@fudan.edu.cn (X.Z.)
xujianqing@fudan.edu.cn (J.X.)

Highlights

GPI-anchored LY6E constrains a negative regulatory mechanism controlling LPS signaling

LY6E promotes the ubiquitination and proteasomal degradation of CD14

PHB1 is required for the LY6E-mediated downregulation of CD14

TRIM21 E3 ligase is responsible for the LY6E-mediated ubiquitination of CD14

Zhu et al., iScience 26, 106808
June 16, 2023
https://doi.org/10.1016/j.isci.2023.106808

iScience

CellPress
OPEN ACCESS

Article

A LY6E-PHB1-TRIM21 assembly degrades CD14 protein to mitigate LPS-induced inflammatory response

Xinyu Zhu,[1,3] Linxia Zhang,[1,3] Daobin Feng,[1] Lang Jiang,[1] Peng Sun,[1] Chen Zhao,[1,*] Xiaoyan Zhang,[1,2,*] and Jianqing Xu[1,2,4,*]

SUMMARY

A major theme of host against invading pathogens lies in multiple regulatory nodes that ensure sufficient signals for protection while avoiding excessive signals toward over-inflammation. The TLR4/MD-2/CD14 complex receptor-mediated response to bacterial lipopolysaccharide (LPS) represents a paradigm for understanding the proper control of anti-pathogen innate immunity. In this study, we studied the mechanism by which the glycosylphosphatidylinositol (GPI)-linked LY6E protein constrains LPS response via downregulating CD14. We first showed that LY6E downregulated CD14 via ubiquitin-dependent proteasomal degradation. The subsequent profiling of LY6E protein interactome led to the revelation that the degradation of CD14 by LY6E requires PHB1, which interacts with CD14 in a LY6E-dependent manner. Finally, we identified the PHB1-interacting TRIM21 as the major ubiquitin E3 ligase for the LY6E-mediated ubiquitination of CD14. Together, our study elucidated the molecular basis of LY6E-mediated governance of LPS response, alongside providing new insights to regulatory mechanisms controlling the homeostasis of membrane proteins.

INTRODUCTION

Inflammation is a fundamental immune response involved in defense against inside and outside challenges.[1] However, once dysregulated inflammatory response can turn to be pernicious, resulting in tissue damages and in severe cases even deaths. An inflammatory response is deemed to be a multi-step process, well demonstrated by the development and the control of host innate immunity against evading pathogens, among which the TLR4-mediated LPS response represents one of the best understood paradigms. TLR4, a surface transmembrane receptor belonging to the evolutionarily conserved toll-like receptor (TLR) family, is specialized in recognition of LPS from Gram-negative bacteria and preferentially expressed in innate immune cells, such as monocytes/macrophages.[2] One remarkable feature of TLR4-LPS engagement is the involvement of multiple ancillary factors (co-receptors) including LPS binding protein (LBP), CD14, and MD2, LBP accounts for the initial capturing of LPS, which is then transferred to CD14 for delivery to TLR4/MD2 complex, within which MD2 cooperate with TLR4 in LPS binding, thereby facilitating the dimerization of TLR4/MD2/LPS complexes that initiate the signal transduction from the plasma membrane. It has been postulated that such stepwise binding of LPS by multiple factors is designed to maximize efficiency in recognizing LPS with each step lowering the threshold of LPS that is sufficient for recognition by the next step. Interestingly, recent studies revealed that CD14 also promotes the endocytosis of TLR4/MD2/LPS complexes, driving a switch from cell surface signaling, which culminates in the activation of NF-κB through the myddosome to upregulate the transcription of inflammatory cytokines, to endosomal signaling, which triggers the formation of a Toll/IL-1R domain-containing adapter-inducing interferon-β (TRIF)-dependent complex, TRIFosome, allowing for the activation of IRF-3 pathway to induce the production of type I interferon.[3–5] Thus, CD14 appears to sit at the apex of TLR4 signaling, required not only for LPS delivery but also for the downstream intracellular signaling, though itself is not a part of the TLR4 signaling complex.

Interestingly, CD14 is also a phenotype marker of monocytes, which circulate in the peripheral blood and serves as a major effector cells of innate immune system and inflammatory response. As a heterologous population, human monocytes are divided into three different subsets according to the expression levels

[1]Shanghai Public Health Clinical Center & Institutes of Biomedical Sciences; Fudan University, Shanghai 201508, P. R. China

[2]Clinical Center of Biotherapy, Zhongshan Hospital, Fudan University, Shanghai 200032, P. R. China

[3]These authors contributed equally

[4]Lead contact

*Correspondence: chen_zhao72@163.com (C.Z.), zhangxiaoyan@fudan.edu.cn (X.Z.), xujianqing@fudan.edu.cn (J.X.)

https://doi.org/10.1016/j.isci.2023.106808

of CD14 and CD16: classical $CD14^{hi}CD16^{-}$subset, intermediate $CD14^{hi}CD16^{+}$ subset, and non-classical $CD14^{+}CD16^{hi}$ subset.[6] During the steady state, $CD14^{hi}CD16^{-}$subset constitutes the majority of monocytes while $CD14^{+}CD16^{hi}$ subset only presents as a minor subpopulation. The expanding of $CD14^{+}CD16^{hi}$ subset has been reported in system lupus erythematosus,[7] rheumatoid arthritis,[8] atherosclerosis,[9] and HIV-1 infection.[10] Moreover, a recent single-cell analysis revealed a unique monocyte subpopulation in severe COVID-19 patients, characterized by enriched expression of inflammation-related genes.[11] Thus, dysregulation of inflammatory monocytes might be relevant to various pathological conditions, particularly in the cases where the inflammatory cytokines are overproduced, a phenomenon often vividly terms as ''cytokine storm''.

Consistent with the importance of a balanced inflammatory response, a growing list of molecules have emerged of inhibitory roles in different inflammation-related signaling pathways. In this context, we previously identified lymphocyte Ag 6 complex, locus E (LY6E), a GPI-anchored surface protein, as a new negative regulator of TLR4 signaling. Such identification stemmed from the finding that LY6E were evidently upregulated in all subsets of monocytes in HIV patients compared with those in healthy control.[12] This upregulation is likely ascribed to sustained activation of type I signaling associated with persistent HIV infection as LY6E showed potent induction in human THP-1 monocyte cell line in response to IFN treatment, qualifying it as an interferon-stimulated gene (ISG). With the demonstration that LY6E attenuates the monocyte responsiveness via downregulation of CD14 expression, we postulated that upregulation of LY6E is a gating mechanism of CD14/TLR4 pathway; its operation in monocytes in HIV patients is critical in the context of co-infection with Gram-negative bacteria, which often occurs in HIV patients, where monocytes face the risk of exposure to bacteria-derived LPS that translocate from gastrointestinal tract owing to impaired mucosal integrity. Without LY6E regulation, excessive inflammation might be induced, resulting in manifestation of clinical phenotypes including tissue damages and possibly viral dissemination.

It should be noted that LY6E is more than a regulator of inflammatory response. LY6E is historically linked to T cell activation after its delineation as a thymocyte marker to discern mature from immature thymocytes,[13] and later experiments indeed found that LY6E positively regulate T cell receptor (TCR) signaling.[14] LY6E have also been implicated in regulation of other biological processes, such as cell adhesion and[15] cancer progression.[16] An aspect of LY6E biology that recently attracts extensive interests is its involvement in various viral infection. Depending on the virus, LY6E could exert a negative, positive, or complex effect on viral infection. The list of viruses showing dependence of LY6E in enhanced susceptibility includes avian Marek's disease virus (MDV),[17] mouse adenovirus type 1 (MAV-1),[18] and flavivirus.[19] In the case of flavivirus, LY6E promotes viral entry through assembling microtubule-like structures, consisting with a selective role in the internalization of large cargo.[19] On the other hand, LY6E functions as a cognate anti-viral ISG in inhibiting the infection of human Coronaviruses including SARS-CoV-2, and the inhibition is attributed to interruption of spike protein mediated membrane fusion.[20] Of interest, LY6E has been proposed to differentially impact HIV infection of CD4 cells depending on the integration of two opposite LY6E activities, i.e., decreasing surface level of CD4 by promoting its internalization versus enhancing viral membrane fusion, which, respectively, inhibits and enhances virus uptake.[21,22] Thus, LY6E plays a plethora of physiological roles, but the underlying mechanisms remains largely unclear concomitant with a poor knowledge about LY6E-associated proteins.

In this study, we sought to determine the molecular mechanisms by which LY6E-downregulates CD14 expression. We show that LY6E mainly inhibited CD14 expression via promoting ubiquitin-dependent proteasomal degradation of CD14 protein. The subsequent interrogation of LY6E-interacting proteins led to the identification of PHB1 as an essential partner of LY6E in degrading CD14. Importantly, we were able to uncover TRIM21 as the major E3 ligase downstream of PHB1 that is responsible for CD14 degradation. These findings provide new insights into the molecular basis of the immunomodulatory activities of LY6E.

RESULTS

LY6E inhibits CD14 protein expression and LPS-induced inflammatory response

Our previous study showed that reduced CD14 level was correlated with upregulation of LY6E in monocytes from patients with chronic HIV infection.[12] We sought to explore the potential mechanisms by which LY6E downregulates CD14. To facilitate this mechanistic exploration, we generated two N-terminal tagged versions of LY6E, namely 3F-LY6E (briefed as 3F-L) and 3F-S-LY6E (briefed as 3F-S-L), by respectively inserting a 3×FLAG and a 3×FLAG plus S-tag sequence in frame between the 23rd and 24th amino acid of LY6E

coding sequence without disturbing the signal peptide. To rule out the possibility that such N-terminal tagging might influence the protein properties of LY6E, we characterized the cellular localizations of 3F-S-L as a representative of the two versions by multiple assays. When 3F-S-L was expressed in THP-1 cells by transduction with a lentiviral expression vector, fractionation experiment showed that it was nearly exclusively distributed in the membrane fraction (Figure S1A). We further verified the identity of 3F-S-L as a GPI-anchored membrane protein by assaying its susceptibility to phosphoinositide-specific phospholipase C (PI-PLC), an enzyme specialized in cleavage of GPI tail, and its extractability by Triton X-100 as GPI proteins are known to enrich within the lipid rafts and thus resistant to Triton X- solubilization. To this end, we used HEK-293T cells to express 3F-S-L by transient plasmid transfection. The analyses of transfected cells showed that the expressed 3F-S-L was readily removed by PI-PLC treatment (Figure S1B) while also showing resistance to Triton X-100 extraction (Figure S1C). Together, these results supported that our N-terminal tagging approach of LY6E preserve its GPI anchoring properties.

We examined the effect of changing LY6E level, knockdown by shRNA or overexpression, on mRNA and protein levels of CD14 in THP-1 cells. Both shRNA knockdown and overexpression were performed with retroviral vectors and for the latter; the 3F-L encoding retroviral vector was used. Consistent with previous study, we detected a negative correlation between LY6E and CD14 protein levels, evidenced by that LY6E knockdown led to an increased expression of CD14 (Figure 1A) and that its overexpression was associated with a decreased CD14 protein level (Figure 1B). The ability of 3F-L to inhibit CD14 expression further corroborated our notion that the activities of LY6E are highly likely unaffected by the N-terminal tagging. We subsequently focused on 3F-L-overexpressing cells for further characterization. Compared to empty vector transduced cells, 3F-L-overexpressing cells displayed significantly decreased cell surface level of CD14 measured by flow cytometry, in terms of both percentage of positive cells and mean fluorescence intensity (MFI), and a similar difference was observed with LPS-stimulated cells (Figure 1C). Of interest, measurements of CD14 mRNA by quantitative RT-PCR showed no significant difference between 3F-L-overexpressing and control cells (Figure 1D). These data indicated that LY6E inhibits the expression of CD14 mainly at protein, rather than mRNA, level.

CD14 is essential for LPS-TLR4 pathway by facilitating LPS delivery to the TLR4/MD2 complex and controlling the endocytosis of TLR4 following the LPS triggering. We thus, speculated that the LY6E-prompted inhibition of CD14 could potentially attenuate the responsiveness of monocytes to LPS stimulation. Consequently, we compared the LPS-induced responses between LY6E-overexpressing cells and control cells. Compared to control cells, the levels of proinflammatory cytokines (TNF-α, IL-6, IL-8, and IL-1β) in the supernatants of LY6E-overexprssing cells were significantly reduced (Figure 1E). The LY6E-mediated reducing effect on the production of proinflammatory cytokines was also reflected by mRNA levels (Figure S2). NF-κB transcriptional factor, in dimeric forms, plays a key role in controlling the transcription of proinflammatory cytokines. The canonical NF-κB dimers, comprising p65 and p50 subunits, are inactive in unstimulated cells due to cytoplasmic sequestration by binding to IκB.[23] In LPS-stimulated cells, TLR4 signaling leads to the activation of downstream kinases, which promote the phosphorylation and the subsequent degradation of IκB proteins, thereby, allowing NF-κB dimers to translocate from cytoplasm to nucleus, where they activate transcription. TLR4 signaling also modulates the activity of NF-κB dimers via stimulating the phosphorylation of the p65 subunit. The LPS-induced phosphorylation of IκBα and NF-κB p65 were both reduced in LY6E overexpressing cells, consistent with an inhibition of TLR4 signaling (Figure 1F). Not only is CD14 required for TLR4 signaling from the cell surface, but also it plays an essential role in the endocytosis of TLR4. Endosomal TLR4 transduces signals through TRIF adaptor protein to activate IRF-3 for transcriptional upregulation of type I interferons (IFNs) and RANTES (regulated upon activation, normal T cells expressed and secreted).[24] Thus, we also examined the impact of LY6E overexpression on the LPS-mediated induction of IFN-α mRNA. As expected, the upregulation of IFN-α mRNA in response to LPS treatment was suppressed in 3F-L-expressing THP-1 cells compared to control cells (Figure 1G). Together, these data supported the notion that LY6E restrains LPS-induced inflammatory response through downregulation of CD14 protein.

LY6E promotes the ubiquitination of CD14

Ubiquitination-mediated proteasomal degradation represents a major way to govern protein homeostasis. We thus, sought to determine whether proteasomal degradation is involved in LY6E-mediated degradation of CD14. To this end, the LY6E overexpressing THP-1 cells were treated with DMSO or MG132, a proteasome inhibitor, and then analyzed for surface expression of CD14 by flow cytometry. The inhibition

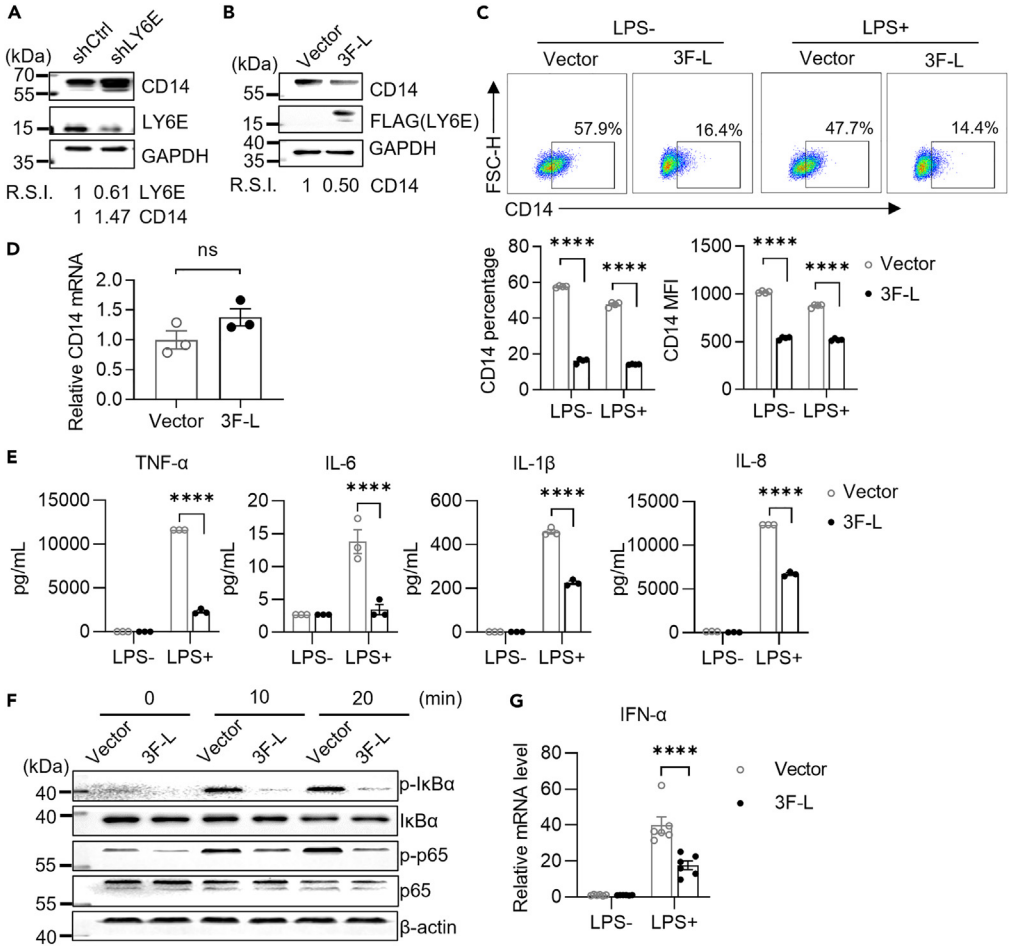

Figure 1. LY6E downregulates CD14 protein expression and attenuates the LPS-induced inflammatory response

(A) THP-1 cells were infected with lentivirus encoding control or LY6E-specific shRNA and subjected to immunoblotting analysis of CD14, LY6E and GADPH as the loading control. R.S.I., relative signal intensity (normalized to values of GADPH). (B–G) THP-1 cells stably expressing 3×FLAG-tagged LY6E (3F-L) or empty vector cells, denoted as 3F-L vs. vector cells, were generated by infecting THP-1 cells with either empty or 3F-L-encoding lentiviral vector with GFP marker, followed by selection of single GFP-positive cells by fluorescence-activated cell sorting (FACS) 7 days post infection and subsequent clonal expansion. The resulting stable cell lines were assured for protein expression by immunoblotting analyses and purity by FACS assessments. (B) 3F-L and vector cells were analyzed for the expression of CD14 and 3F-L by immunoblotting, with GADPH used as the loading control. (C) 3F-L and vector cells, after LPS treatment (100 ng/mL, 6 h), were stained with CD14-APC and analyzed by flow cytometry. Shown are representative flow cytometric plot (**top**) and aggregated data (**bottom**) on the percentage of CD14-positive cells and mean fluorescence intensity (MFI) of CD14 (n = 4; ****, $p < 0.0001$; two-way ANOVA). (D) Comparison of CD14 mRNA levels, determined by quantitative RT-PCR using GADPH as internal control, between Vector and 3F-L cells (n = 3; ns, no significance, $p > 0.05$; t tests). (E) Comparison of proinflammatory cytokine production between LPS-stimulated Vector and 3F-L cells. Cells were treated with mock or LPS (100 ng/mL) for 6 h, and the presence of indicated cytokines in culture supernatants were then analyzed by cytometric bead array (CBA) (n = 3; ****, $p < 0.0001$; two-way ANOVA). (F) Comparison of the activation of NF-κB, as indicated by phosphorylation of IκBα and NF-κB p65 subunit, between LPS-stimulated vector and 3F-L cells. Total cell lysates were prepared at 0 min, 10 min, and 20 min after LPS treatment and analyzed by immunoblotting with antibodies specific for total and phosphorylated forms of IκBα and NF-κB p65, and β-action as the loading control. (G) Comparison of the LPS-stimulated production of IFN-α mRNA between vector and 3F-L cells. Cells were mock or LPS (1 μg/mL) stimulated for 2 h before harvesting for total RNA extraction, followed by determination of IFN-α mRNA levels by quantitative RT-PCR, which are expressed as fold-of-induction relative to untreated cells (n = 6; ****, $p < 0.0001$; two-way ANOVA).

on CD14 surface expression by LY6E was largely rescued by the presence of MG132. The significant upregulation of CD14 surface level by MG132 in the vector group, though less pronounced than the LY6E overexpressing cells, indicated that proteasomal degradation of CD14 took place in resting normal

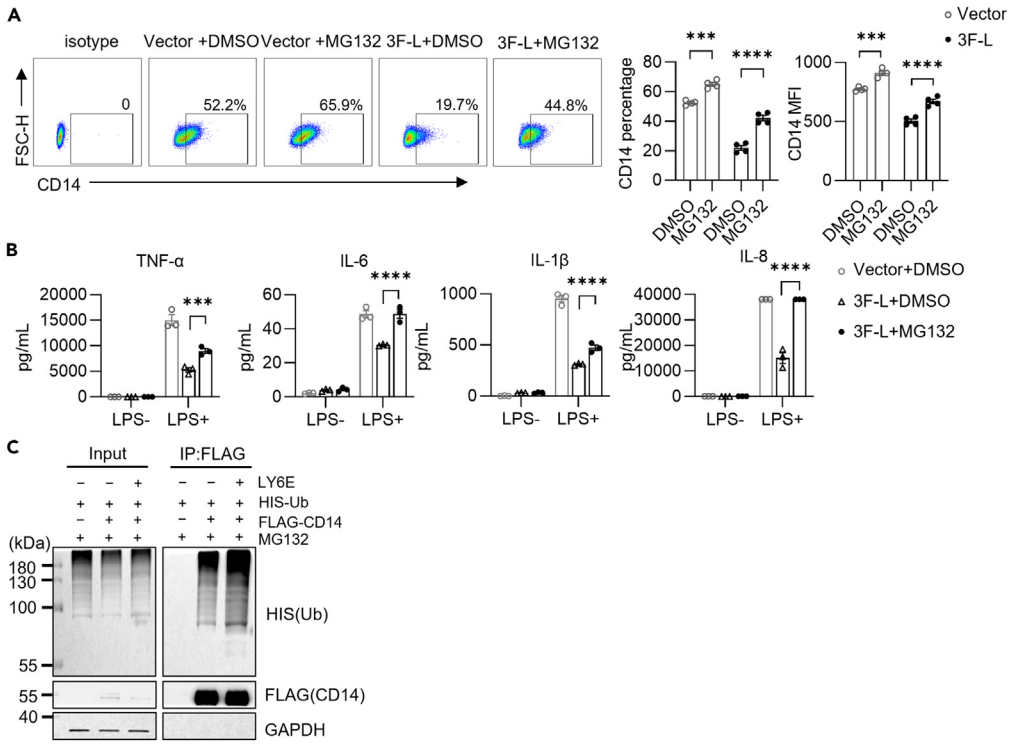

Figure 2. LY6E promotes the ubiquitination and proteasomal degradation of CD14

(A) 3×FLAG-LY6E (3F-L) overexpressing or control (Vector) THP-1 cells, described in Figure 1, were treated with MG132 (10 μM) or DMSO for 18 h before subjecting to flow cytometry to assess CD14 surface levels. Shown in left and right are representative flow cytometric plot and aggregate data on the percentage of CD14 positive cells and the MFI of CD14, respectively (n = 4; ***, $p < 0.001$; ****, $p < 0.0001$; two-way ANOVA).

(B) The same cells in (A), after pretreatment with MG132 (10 μM) or DMSO for 12 h, were subjected to LPS (100 ng/mL) treatment for 6 h. The culture supernatants were then analyzed by CBA to determine the levels of indicated cytokines (n = 3; ***, $p < 0.001$; ****, $p < 0.0001$; one-way ANOVA).

(C) Assessments of LY6E-mediated ubiquitination of CD14. HEK-293T cells stably expressing non-tagged LY6E or control (empty vector) cells, generated by lentiviral vector-mediated infection and clonal selection follows procedures as described in Figure 1, were co-transfected with a plasmid encoding His-tagged ubiquitin and a plasmid encoding an N-terminally FLAG-tagged CD14, FLAG-CD14. After 48 h' further culturing, the cells were treated MG132 (10 μM) for 6 h before collecting to prepare cell lysates, which were then selected by anti-FLAG resin. The bound proteins were eluted by 3×FLAG peptide and analyzed together with the inputs by immunoblotting analyses with the indicated antibody.

THP-1 cells (Figure 2A). MG132 treatment also markedly enhanced the production of secreted proinflammatory cytokines by LY6E overexpressing cells in response to LPS stimulation (Figure 2B).

We then examined whether LY6E affects the ubiquitination of CD14. To facilitate this examination, we utilized an N-terminally FLAG-tagged CD14 version, FLAG-CD14, which allows effective immunoprecipitation. For validating the use of FLAG-CD14, we performed transient plasmid transfection to express FLAG-CD14 in HEK-293T cell, which lacks endogenous CD14 expression (Figure S3A), and analyzed the expressed FLAG-CD14 proteins using assays that were essentially the same as described above for characterization of 3F-S-L protein. Fractionation experiments characterized FLAG-CD14 as a membrane associated protein (Figure S3B). Also, FLAG-CD14-expressing cells were detected positively for both FLAG and CD14 staining by flow cytometry without cellular permeabilization (Figure S3A), verifying the cell surface expression of FLAG-CD14. Furthermore, FLAG-CD14, behaving similarly to non-tagged CD14, was susceptible to PI-PLC treatment (Figure S3C) and resistant to Triton X-100 extraction (Figure S3D). Importantly, as expected, FLAG-CD14 showed downregulation in response to co-expression of LY6E (Figure S3E). Together, these results justified the suitability of FLAG-CD14 for studying the LY6E-CD14 interaction.

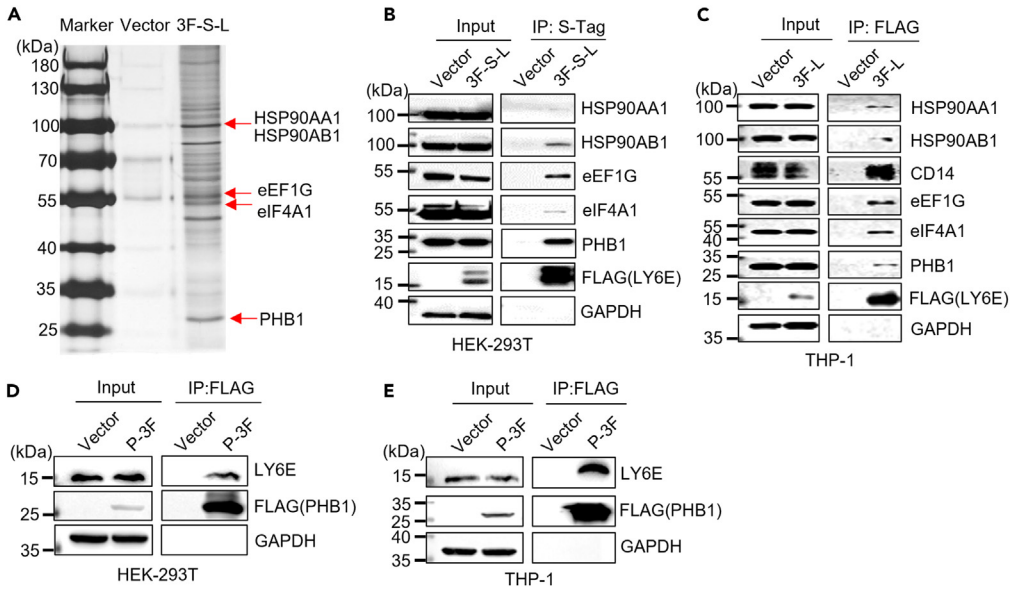

Figure 3. LY6E interactome revealed the associations of LY6E with multiple proteins represented by PHB1

(A) Identification of LY6E interactomes by co-immunoprecipitation coupled with mass spectrometry. HEK-293T cells stably transduced with 3×FLAG-S-tagged LY6E encoding or empty lentiviral vectors, denoted as 3F-S-L and vector cells, were used for prepare cell lysates, which were subjected to sequential selection with anti-FLAG and anti-S-tag affinity gel. The purified immunoprecipitaes were separated by SDS-polyacrylamide gel electrophoresis and revealed by silver staining, followed by cutting out the most stained bands for mass spectrometry analyses. Several proteins were identified with high confidence, their names and the corresponding protein bands were indicated.

(B and C) Validation of the identified LY6E interactome. (B): LY6E immunoprecipitaes obtained from vector or 3F-S-L cells through the same tandem purification procedure as described in (A) were analyzed by immunoblotting with the indicated antibodies. (C): Validation was performed using lysates prepared from vector or 3F-L THP-1 cells described in Figure 1; the lysates were selected with anti-FLAG affinity gel and the resultant immunoprecipitaes together with inputs were probed by the same antibody set used in (B) plus anti-CD14.

(D and E) Reverse pull-down of LY6E by PHB1. HEK-293T cells or THP-1 cells stably expressing C-terminally 3×FLAG tagged PHB1 (P-3F) and control (Vector) cells were generated following the same lentiviral vector-mediated infection and clonal selection procedures as described in Figure 1. Cell lysates were prepared from these cells, subjected to selection with anti-FLAG affinity gel, and the resultant immunoprecipitaes together with inputs were analyzed by immunoblotting for the presence of P-3F, endogenous LY6E, and GADPH as a control: HEK-293T cells in (D) and THP-1 cell in (E).

Ubiquitination assays were performed using HEK-293T cells overexpressing LY6E or control HEK-293T cells, and co-transfection of a plasmid encoding His-tagged ubiquitin with an FLAG-CD14 expressing vector or empty control vector. The co-transfected cells, after exposure to MG132, were used to prepare cell lysates, which were subsequently immunoprecipitated with anti-FLAG resin, followed by FLAG peptide elution. Western blotting analyses of the resultant elutes showed that the ubiquitination of CD14 was dramatically enhanced by LY6E (Figure 2C). This result, together with the above observed rescuing effect of MG132 on CD14 expression, demonstrated that the LY6E promotes the degradation of CD14 via the ubiquitination-proteasome pathway.

LY6E interactome analysis identified PHB1 as a major LY6E-interacting protein

As a GPI-anchored protein, LY6E cannot accomplish the task of ubiquitinating CD14 by itself. To gain insight into LY6E-mediated ubiquitination of CD14, we sought to explore the protein interaction network of LY6E. To facilitate this exploration, we constructed HEK-293T cells stably expressing the N-terminally double-tagged LY6E, 3F-S-L, which was described and characterized above. These cells were denoted as 3F-S-L cells. Cell extracts from 3F-S-L cells were subjected to sequential selection with anti-FLAG and anti-S-Tag resin. The purified proteins were then separated by denaturing SDS electrophoresis, followed by silver staining. Figure 3A shows the stained gel, indicating that a significant number of proteins were co-purified with LY6E. To identify the major interacting proteins, we cut out the most intense bands from the gel and subjected them to mass spectrometry analysis. Five candidate proteins, namely HSP90AA1, HSP90AB1, eEF1G, eIF4A1, and PHB1, were identified with high confidence, and we validated

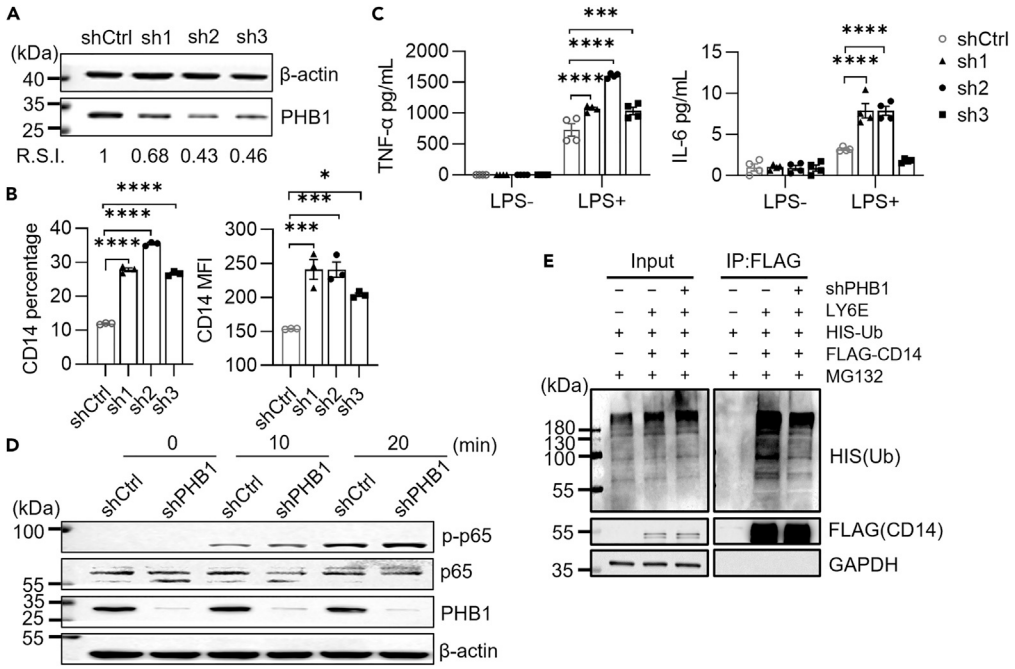

Figure 4. PHB1 is required for LY6E-mediated ubiquitination and degradation of CD14, and the inhibition of LPS responsiveness

(A) Knockdown efficacy of PHB1 by shRNA in THP-1 cells. Three lentiviral vectors were constructed, each expressing a different PHB1-targeting shRNAs (sh1, sh2, and sh3), and together with control shRNA-expressing vector (shCtrl) were individually transduced into THP-1 cells, from which PHB1 expression was determined by immunoblotting.

(B) Impact of PHB1 knockdown on CD14 surface expression. The indicated PHB1-targeting and control shRNA hosting THP-1 cells were analyzed for CD14 surface expression by flow cytometric, in terms of both percentage of CD14 positive cells and MFI (n = 3; *, $p < 0.05$, ***, $p < 0.001$; ****, $p < 0.0001$; one-way ANOVA).

(C) Impact of PHB1 knockdown on LPS-induced proinflammatory cytokine production. Shown in left and right, respectively, are supernatant levels of TNF-α and IL-6 with or without LPS stimulation (100 ng/mL for 6 h), analyzed by CBA (n = 4; *, $p < 0.05$; ****, $p < 0.0001$; two-way ANOVA).

(D) Impact of PHB1 knockdown on LPS-induced activation of NF-κB. THP-1 cells expressing control shRNA (shCtrl) or PHB1-specific shRNA (sh2, denoted as shPHB1) were stimulated with LPS for the indicated time points, and the activation of NF-κB were analyzed by immunoblotting with antibodies against total and phosphorylated p65 subunit.

(E) Effect of PHB1 knockdown on LY6E-mediated CD14 ubiquitination. Ubiquitination of transfected FLAG-CD14 was examined in HEK-293T stably expressing non-tagged LY6E described in Figure 2C, with or without co-expression of shPHB1 (sh2) that was introduced using a lentiviral vector. Detailed procedure is seen in Figure 2C.

their association with LY6E by immunoblotting of protein samples derived from 3F-S-L cells through the same tandem purification procedure (Figure 3B). To exclude the possibility that the identified interactions is context dependent (specific for HEK-293T cells), we repeated the validation experiment using the 3F-L expressing THP-1 cells and all five candidate proteins were found to be co-immunoprecipitated with LY6E, corroborating their identity as members of LY6E interactome (Figure 3C). Notably, we also detected the presence of CD14 in the LY6E immunoprecipitaes (Figure 3C), suggesting that LY6E interacts with CD14.

PHB1 (prohibitin, also known as PHB), a member of the Band-7 family of proteins, was reported to be required for the Ras-mediated activation of C-Raf and modulate adhesion and migration of epithelial cells.[25] PHB1 was also identified as the receptor of Chikungunya virus.[26] These studies suggest a linkage of PHB1 to cell membrane-related biological processes. Thus, we chose PHB1 for further characterization. Before functional exploration, we further confirmed the LY6E-PHB1 interaction by reverse pull-down of Figure 3C using HEK-293T and THP-1 cells stably expressing 3×FLAG-tagged PHB1 (Figures 3D and 3E).

PHB1 is required for LY6E-mediated suppression of CD14 expression

To evaluate the functions of PHB1, we stably infected THP-1 cells with lentiviruses encoding three different PHB1-targeting short hairpin RNAs (denoted as sh1-3). Compared to control THP1 cells, PHB1 shRNA-expressing cells concomitantly showed reduced level of PHB1 proteins, demonstrating targeting efficacy (Figure 4A), and increased surface CD14 protein expression, as judged by flow cytometry analyses (Figures 4B and S4A). Consistent with the improved expression of CD14 that could lead to enhanced TLR4 signaling, these cells were also characterized by enhanced production of proinflammatory cytokines (TNF-α and IL-6) (Figure 4C), and elevated phosphorylation of NF-κB p65 (Figure 4D). Thus, PHB1, like LY6E, negatively regulates the CD14 protein expression and suppresses the responsiveness to LPS.

To determine the functional relationship between PHB1 and LY6E, we analyzed the requirement of PHB1 for LY6E-mediated CD14 downregulation. We found that silencing of PHB1 by shRNA could largely rescue the decrease in surface CD14 expression exhibited by LY6E-overexpressing THP1 cells (Figure S4B), as well as the reduced secretion of TNF-α (Figure S4C). Next, we addressed whether PHB1 is involved in the enhanced ubiquitination of CD14 caused by LY6E. Ubiquitination assays were performed using LY6E overexpressing HEK-293T cells that were infected with control or PHB1 shRNA lentiviral vector. PHB1 shRNA-expressing cells showed a marked reduction in the ubiquitination of CD14 compared to control cells (Figure 4E). These results together demonstrated that PHB1 acts downstream of LY6E in promoting the ubiquitination and degradation of CD14.

TRIM21 is the primary E3 ligase, recruited by PHB1, for LY6E-mediated CD14 ubiquitination

In the process of ubiquitination, the target specificity is determined by E3 ubiquitin ligases, which recognize the substrates and account for transferring ubiquitin from E2 enzymes to substrates. We sought to identify the E3 ligase utilized by LY6E to ubiquitinate CD14. No E3 ligase was found among the major LY6E associated proteins identified by aforementioned mass spectrometry analyses of LY6E immunoprecipitaes. PHB1 is known as a scaffold protein, thus, it is likely that PHB1 may provide the docking platform for the recruitment of the E3 ligase. Two E3 ligases, SKP2, and TRIM21, have been documented as PHB1-binding proteins.[27,28] Therefore, we investigated their interactions between CD14 by co-immunoprecipitation. The result revealed that although both TRIM21 and SKP2 were detectably co-immunoprecipitated with CD14, the amount of TRIM21 co-precipitated was significantly higher than that of SKP2 co-precipitated (Figure 5A). Notably, the association between TRIM21 and CD14 showed a dependence on both LY6E and PHB1 as it was enhanced by LY6E overexpression and this enhancement was attenuated upon PHB1 silencing. In contrast, the CD14-SKP2 association was not affected by changes in LY6E or PHB1 (Figure 5A). These data inferred that TRIM21 might be the E3 ligase for LY6E-mediated ubiquitination of CD14. To substantiate this inference, ubiquitination assays were performed in the LY6E-overexpressing HEK-293T cells upon silencing of TRIM21 or SKP2. The knockdown of TRIM21, but not SKP2, resulted in a weakened ubiquitination of CD14 (Figures 5B and S5). Consistent with that ubiquitination is a requisite for LY6E-mediated degradation of CD14, the suppressed surface CD14 expression in LY6E overexpressing cells was relieved by TRIM21 knockdown to a large extent (Figure 5C). Collectively, these data solidified the role of TRIM21 as the primary E3 ligase responsible for CD14 ubiquitination initiated by LY6E.

To explore the organization of LY6E, PHB1, and TRIM21 in the process of CD14 ubiquitination, we examined the LY6E dependency of PHB1 in interacting with CD14. Using co-immunoprecipitation analyses, we found that LY6E knockdown attenuated the association of PHB1 with CD14, whereas its overexpression strengthened such association (Figure 5D). This result, combined with the fact that TRIM21 binds to PHB1, led us to propose that LY6E acts as the bridge to connect CD14 to PHB1, which subsequently recruits TRIM21 to target CD14 for proteasomal degradation via ubiquitination.

DISCUSSION

The CD14/MD2/TLR4-mediated LPS signaling provide a paradigm for understanding how inflammatory response is handled to attain a level or duration of inflammation that is adequate for a protective effect, e.g., resolution of infection, without introducing adverse effects seen in the occurrence of overshooting. Not surprisingly, the exploration of TLR4 signaling network reveals the existence of intrinsic negative regulation, wherein multiple steps ranging from cell surface receptor level to the assembly of downstream signaling complex are subjected to tight control. An important part of this regulation is feedback

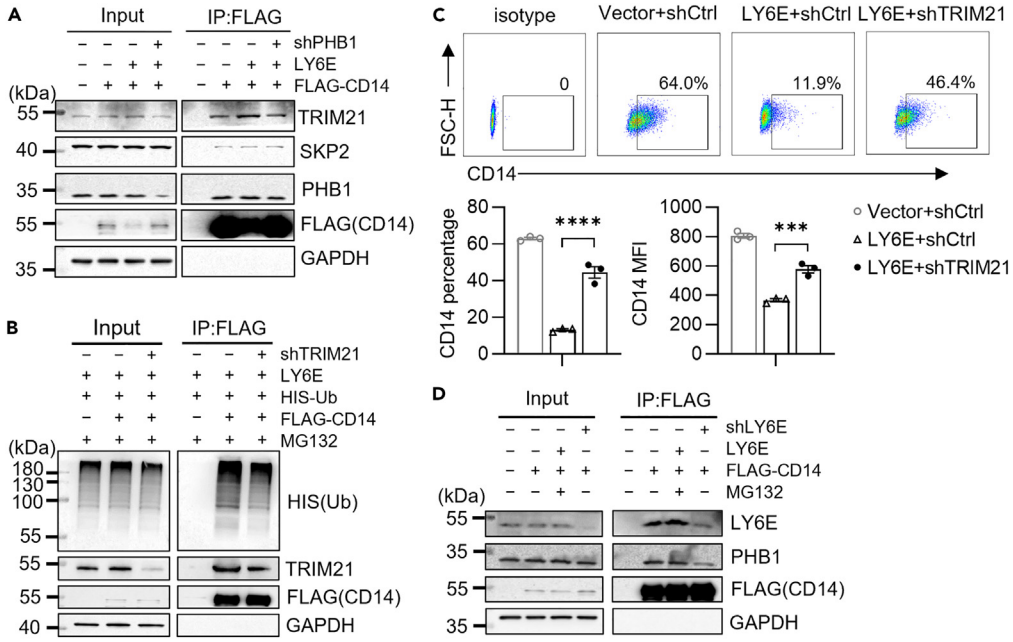

Figure 5. TRIM21 is the primary E3 ligase recruited by PHB1 to participate in the LY6E-meidated ubiquitination of CD14

(A) PHB1-mediated connection between CD14 and a ubiquitin E3 ligase. HEK-293T cells stably expressing non-tagged LY6E or control cells described in Figure 2C were infected with control shRNA or PHB1-specific shRNA (sh2, denoted as shPHB1) encoding lentiviral vector, prior to transfection with a plasmid expressing FLAG-CD14 or an empty plasmid. The cells were used for preparation of cell extracts that were subjected to selection by anti-FLAG affinity gel, and the resultant immunoprecipitaes were analyzed for the presence of the indicated proteins, including two known PHB1-interacting E3 ligases, SKP2 and TRIM21, by immunoblotting.

(B) Determination of the role of TRIM21 in LY6E-mediated CD14 ubiquitination. The effect of the expression of TRIM21-specific shRNA (shTRIM21) on the ubiquitination of transfected FLAG-CD14 was evaluated in the HEK-293T cells stably expressing non-tagged LY6E, using the procedures detailed in Figure 2D.

(C) Examination of TRIM21 dependency of LY6E-mediated CD14 suppression in THP-1 cells. LY6E-overexpressing THP-1 cells were enforced to express control shRNA (shCtrl) or TRIM21-specific shRNA (shTRIM21) by lentiviral vector infection, and analyzed for CD14 surface expression by flow cytometry. Shown are representative flow cytometric plots (**top**) and aggregate data (**bottom**) on the percentage of CD14 positive cells and MFI (n = 3; ****, $p < 0.0001$; one-way ANOVA).

(D) Dissection of the relationship of LY6E and PHB1 in interacting with CD14. Wild-type HEK-293T were infected with an empty lentiviral vector or vectors encoding either a LY6E-targeting shRNA (shLY6E) or non-tagged LY6E, and subsequently mock transfected or transfected with an FLAG-CD14 expression plasmid. The cells were analyzed for the association between CD14 and LY6E, PHB1 by anti-FLAG co-immunoprecipitations followed by immunoblotting with the indicated antibodies. Cells under LY6E overexpression were also treated with MG132 to stabilize the co-expressed CD14 proteins.

mechanisms that utilize TLR signaling to directly or indirectly upregulate negative regulators, which in turn serves to antagonize inflammatory response.[29] For example, IL-10 produced from TLR-ligand-stimulated cells could act backwardly to restrain the production of inflammatory cytokine.[30] Another example is demonstrated by EP4-mediated negative regulation of TLR4 endocytosis, which is required for the activation of the TRIF branch.[31] Such regulation is primed by TLR4 signaling, which stimulates the production and secretion of prostaglandin E2 (PGE2), consequently promoting the activation of the PGE2 receptor EP4. Here, we uncovered a new layer of control of LPS response that channels through the GPI-anchored LY6E protein. Our results elucidated the mode of anti-inflammatory action of LY6E, which is LY6E binds to CD14 and targets it for ubiquitination and proteasomal degradation in both resting and LPS-treated cells. We further identified two essential partners of LY6E involved in this action, PHB1, which is recruited to CD14 thorough LY6E, and TRIM21, which is a ubiquitin E3 ligase interacting with PHB1 and is required for CD14 ubiquitination. Given the central role of CD14 in LPS-mediated activation of TLR4 receptor, by reducing the surface expression of CD14, LY6E attenuates the downstream intracellular signal transduction, thus restraining the activation of NF-κB and the production of inflammatory cytokines.

Using both LY6E-overexpressing and knockdown cells, we provided strong evidences demonstrating that LY6E downregulates CD14 through a ubiquitination-proteasome pathway. The first indication came from the finding that LY6E affected CD14 mainly at the protein level rather than at the mRNA level. We were able to further show that LY6E significantly enhanced the ubiquitination of CD14 and more importantly, LY6E-mediated CD14 downregulation and attenuation of LPS response could be largely rescued by the proteasomal inhibitor MG132.

Given the nature of LY6E as a GPI-anchor protein without intracellular domain mediating signal transduction, we postulated that LY6E-mediated biological processes involve other proteins capable of transmitting a signal to the inside of cells, which could be recruited by LY6E by protein-protein interaction. We thus, utilized co-immunoprecipitation and mass spectrometry to decipher protein interaction network of LY6E, and consequently identified PHB1 as a major LY6E-interacting protein. The subsequent analyses of LPS responsiveness of PHB1 knockdown cells revealed that decreasing PHB1 concomitantly enhanced the expression of CD14, the phosphorylation of NF-κB p65, and the production of inflammatory cytokines. We further showed that PHB1 knockdown inhibited the LY6E-mediated ubiquitination of CD14, which, in combination with the observation that the PHB1-CD14 association was positively correlated with the protein level of LY6E, indicated that LY6E acts as a bridge between PHB1 and CD14. Of interest, PHB1 was previously reported to suppress NF-κB activation in intestinal epithelial cells and nasopharyngeal carcinoma cells.[27,28] It awaits further investigation whether its partnership with LY6E is also required in those contexts.

Besides PHB1, we identified several proteins associated with LY6E. HSP90AA1 and HSP90AB1 are molecular chaperons involved in protein folding and the activation of disparate client proteins that have key roles in stress response[32,33]; eIF4A1 and eEF1G are critical components of protein translational machinery, serving in the initiation and elongation step, respectively. How these associated proteins affect the activities of LY6E remain to be explored. They could be organized into a super-complex that functions a signaling hub or they belong to different complexes specialized in different LY6E functionalities.

Our exploration of LY6E-mediated CD14 degradation ends in the identification of the responsible E3 ligase, TRIM21. This identification was facilitated by the recognition of PHB1 as a scaffold protein, which suggest that PHB1 could possibly acts as an adaptor to bring a E3 ligase to CD14. Allowing for this possibility, we tested two known PHB1-interacting E3 ligase, TRIM21 and SKP2, and found that only TRIM21 interacted with CD14 in a PHB1-dependent manner. The candidacy of TRIM21, as the E3 ligase mediating CD14 degradation by LY6E-PHB1 complex was strengthened by the findings that TRIM21 knockdown largely concomitantly reversed the effect of LY6E overexpression on the ubiquitination and expression of CD14. Interestingly, we also detect a weak, PHB1-independent association between SKP2 and CD14, and its biological relevance is not yet clear.

Together, the above results lead us to propose that LY6E-mediated CD14 downregulation is a highly orchestrated event driven by ordered protein-proteins: LY6E directly binds to CD14 and likely also PHB1, thus bridging PHB1 to CD14, followed by the recruitment of TRIM21 by PHB1 for targeting CD14 to ubiquitination and proteasomal degradation. It remains open whether this event involves additional factors. For example, the interaction between LY6E and CD14, both of which are GPI-anchored protein, might be facilitated by their lipid raft localization. A real challenging question is how the LY6E-PHB1-TRIM21 assembly achieve outside-to-inside communication, with LY6E and the CD14 targets located outside of the cells whereas TRIM21 and the ubiquitin-proteasome residing in the cytoplasm. It is generally accepted that the degradation of surface proteins exclusively relies on the endocytosis-lysosome pathway. Indeed, previous studies already implicated a connection between LY6E and endocytic process of protein and virus, and surface level of CD14 is known to be regulated by endocytosis. However, supposing that CD14 proteins reach the inside of cell through endocytosis-mediated internalization, it would be sequestered in the endosomal vesicle, thus requiring an escaping mechanism to get access to TRIM21 and/or proteasome. An alternative, provocative hypothesis is that CD14 is transported into cytoplasm by a, yet, unidentified mechanism that is independent of endocytosis. No matter what internalization route CD14 takes, that process is most likely gated by PHB1. A remarkable property of PHB1 is that it is capable of heterodimerizing with PHB2, the other member of PHB protein family, to build up a PHB1:PHB2 ring structure. The PHB1:PHB2 complex plays a key role in mitochondria homeostasis by acting as a scaffold or platform that modulates the folding, stability, and assembly of newly imported proteins.[34] Similar function might be

performed by surface membrane associated PHB complex, if true, CD14 could just be the first example of membrane proteins whose turnover or stability is governed by this complex. A recent study lent support for this view, suggesting that cell surface PHB proteins play a critical role in modulating the TH17 polarization and pathogenicity.[35]

In summary, by uncovering LY6E-PHB1-TRIM21 as a protein assembly targeting CD14 for ubiquitination-dependent proteasomal degradation, the present study not only establish a new negative regulatory mechanism of LPS signaling, but also provides novel insights regarding the molecular pathways that regulate the homeostasis of cell surface proteins. Besides, the proteomic analysis of LY6E protein network is expected to land a new foundation for a better understanding of LY6E biology and its role in diseases. Finally, given the key roles of CD14 in TLR4-mediated signaling and under- and over-inflammation have been associated with unfavorable physiological outcomes; LY6E-PHB1-TRIM21 assembly may represent a new target for inflammation-related drug development. The architecture of LY6E-PHB1-TRIM21 assembly naturally resembles the PROTAC design, with LY6E serving the ligand for the point-of-interest and PHB1 the ligand for the E3 ligase. The rewiring of this complex or identification of small molecules targeting this complex for functional enhancement or disruption is certainly warranted for future exploration toward new effective therapeutics against infectious and inflammatory diseases.

Limitations of the study

One caveat of our study is that we mainly performed experiments on one human monocyte cell line, THP-1. Further examinations using human primary monocyte/macrophage cells, alongside analyses of LPS response in a mouse model, would be required to reinforce our conclusion that LY6E-PHB1-TRIM25 acts as a general, critical axis governing the LPS response through CD14 downregulation. Lastly, the relevance of our findings to human diseases, e.g., pathophysiological conditions caused by over-inflammation responding to bacterial infection, awaits future research.

STAR★METHODS

Detailed methods are provided in the online version of this paper and include the following:

- KEY RESOURCES TABLE
- RESOURCE AVAILABILITY
  - Lead contact
  - Materials availability
  - Data and code availability
- EXPERIMENTAL MODEL AND SUBJECT DETAILS
  - Cell lines
  - Plasmids
- METHOD DETAILS
  - Lentiviral transduction
  - RT-qPCR
  - LPS stimulation
  - PI-PLC treatment
  - Fractionation analyses
  - Immunoblotting
  - Co-immunoprecipitations
  - Ubiquitination assays
  - Flow cytometry analyses
- QUANTIFICATION AND STATISTICAL ANALYSIS
  - Statistical analyses

SUPPLEMENTAL INFORMATION

Supplemental information can be found online at https://doi.org/10.1016/j.isci.2023.106808.

ACKNOWLEDGMENTS

This work was supported by the National Natural Science Foundation of China (82071788, 82072273), the Technology Service Platform for Detecting High level Biological Safety Pathogenic Microorganism

Supported by Shanghai Science and Technology Commission (21DZ2291300), and intramural funding from the Shanghai Public Health Clinical Center.

AUTHOR CONTRIBUTIONS

J.X. conceived the study; X.Z. and L.Z. performed experiments, with assistance from D.F., L.J., and P.S.; L.J. assisted with data analysis; X.Z. wrote the original manuscript; C.Z. revised the manuscript and contributed advice; X.Z. and J.X. supervised the work.

DECLARATION OF INTERESTS

The authors declare no competing interests.

Received: November 16, 2022
Revised: February 2, 2023
Accepted: May 1, 2023
Published: May 4, 2023

REFERENCES

1. Medzhitov, R. (2008). Origin and physiological roles of inflammation. Nature *454*, 428–435. https://doi.org/10.1038/nature07201.

2. Zindel, J., and Kubes, P. (2020). DAMPs, PAMPs, and LAMPs in immunity and Sterile inflammation. Annu. Rev. Pathol. *15*, 493–518. https://doi.org/10.1146/annurev-pathmechdis-012419-032847.

3. Zanoni, I., Ostuni, R., Marek, L.R., Barresi, S., Barbalat, R., Barton, G.M., Granucci, F., and Kagan, J.C. (2011). CD14 controls the LPS-induced endocytosis of Toll-like receptor 4. Cell *147*, 868–880. https://doi.org/10.1016/j.cell.2011.09.051.

4. Rajaiah, R., Perkins, D.J., Ireland, D.D.C., and Vogel, S.N. (2015). CD14 dependence of TLR4 endocytosis and TRIF signaling displays ligand specificity and is dissociable in endotoxin tolerance. Proc. Natl. Acad. Sci. USA *112*, 8391–8396. https://doi.org/10.1073/pnas.1424980112.

5. Tan, Y., Zanoni, I., Cullen, T.W., Goodman, A.L., and Kagan, J.C. (2015). Mechanisms of toll-like receptor 4 endocytosis reveal a common immune-evasion Strategy used by pathogenic and commensal bacteria. Immunity *43*, 909–922. https://doi.org/10.1016/j.immuni.2015.10.008.

6. Rogacev, K.S., Zawada, A.M., Hundsdorfer, J., Achenbach, M., Held, G., Fliser, D., and Heine, G.H. (2015). Immunosuppression and monocyte subsets. Nephrol. Dial. Transplant. *30*, 143–153. https://doi.org/10.1093/ndt/gfu315.

7. Zhu, H., Hu, F., Sun, X., Zhang, X., Zhu, L., Liu, X., Li, X., Xu, L., Shi, L., Gan, Y., and Su, Y. (2016). CD16(+) monocyte subset was enriched and functionally exacerbated in driving T-cell activation and B-cell response in systemic lupus erythematosus. Front. Immunol. *7*, 512. https://doi.org/10.3389/fimmu.2016.00512.

8. Smiljanovic, B., Radzikowska, A., Kuca-Warnawin, E., Kurowska, W., Grün, J.R., Stuhlmüller, B., Bonin, M., Schulte-Wrede, U., Sörensen, T., Kyogoku, C., et al. (2018). Monocyte alterations in rheumatoid arthritis are dominated by preterm release from bone marrow and prominent triggering in the joint. Ann. Rheum. Dis. *77*, 300–308. https://doi.org/10.1136/annrheumdis-2017-211649.

9. Urbanski, K., Ludew, D., Filip, G., Filip, M., Sagan, A., Szczepaniak, P., Grudzien, G., Sadowski, J., Jasiewicz-Honkisz, B., Sliwa, T., et al. (2017). CD14(+)CD16(++) "nonclassical" monocytes are associated with endothelial dysfunction in patients with coronary artery disease. Thromb. Haemostasis *117*, 971–980. https://doi.org/10.1160/th16-08-0614.

10. Prabhu, V.M., Singh, A.K., Padwal, V., Nagar, V., Patil, P., and Patel, V. (2019). Monocyte Based Correlates of Immune Activation and Viremia in HIV-Infected Long-Term Non-progressors, *10*. https://doi.org/10.3389/fimmu.2019.02849.

11. Guo, C., Li, B., Ma, H., Wang, X., Cai, P., Yu, Q., Zhu, L., Jin, L., Jiang, C., Fang, J., et al. (2020). Single-cell analysis of two severe COVID-19 patients reveals a monocyte-associated and tocilizumab-responding cytokine storm. Nat. Commun. *11*, 3924. https://doi.org/10.1038/s41467-020-17834-w.

12. Xu, X., Qiu, C., Zhu, L., Huang, J., Li, L., Fu, W., Zhang, L., Wei, J., Wang, Y., Geng, Y., et al. (2014). IFN-stimulated gene LY6E in monocytes regulates the CD14/TLR4 pathway but inadequately restrains the hyperactivation of monocytes during chronic HIV-1 infection. J. Immunol. *193*, 4125–4136. https://doi.org/10.4049/jimmunol.1401249.

13. Godfrey, D.I., Masciantonio, M., Tucek, C.L., Malin, M.A., Boyd, R.L., and Hugo, P. (1992). Thymic shared antigen-1. A novel thymocyte marker discriminating immature from mature thymocyte subsets. J. Immunol. *148*, 2006–2011.

14. Saitoh, S., Kosugi, A., Noda, S., Yamamoto, N., Ogata, M., Minami, Y., Miyake, K., and Hamaoka, T. (1995). Modulation of TCR-mediated signaling pathway by thymic shared antigen-1 (TSA-1)/stem cell antigen-2 (Sca-2). J. Immunol. *155*, 5574–5581.

15. Classon, B.J., and Boyd, R.L. (1998). Thymic-shared antigen-1 (TSA-1). A lymphostromal cell membrane Ly-6 superfamily molecule with a putative role in cellular adhesion. Dev. Immunol. *6*, 149–156. https://doi.org/10.1155/1998/53157.

16. Yeom, C.J., Zeng, L., Goto, Y., Morinibu, A., Zhu, Y., Shinomiya, K., Kobayashi, M., Itasaka, S., Yoshimura, M., Hur, C.G., et al. (2016). LY6E: a conductor of malignant tumor growth through modulation of the PTEN/PI3K/Akt/HIF-1 axis. Oncotarget *7*, 65837–65848. https://doi.org/10.18632/oncotarget.11670.

17. Liu, H.C., Cheng, H.H., Tirunagaru, V., Sofer, L., and Burnside, J. (2001). A strategy to identify positional candidate genes conferring marek's disease resistance by integrating dna microarrays and genetic mapping. Anim. Genet. *32*, 351–359.

18. Welton, A.R., Chesler, E.J., Sturkie, C., Jackson, A.U., Hirsch, G.N., and Spindler, K.R. (2005). Identification of quantitative trait loci for susceptibility to mouse adenovirus type 1. J. Virol. *79*, 11517–11522. https://doi.org/10.1128/jvi.79.17.11517-11522.2005.

19. Hackett, B.A., and Cherry, S.J. (2018). Flavivirus internalization is regulated by a size-dependent endocytic pathway. Proc. Nat. Acad. Sci. USA *115*, 4246–4251.

20. Pfaender, S., Mar, K.B., Michailidis, E., Kratzel, A., Boys, I.N., V'Kovski, P., Fan, W., Kelly, J.N., Hirt, D., Ebert, N., et al. (2020). LY6E impairs coronavirus fusion and confers immune control of viral disease. Nat. Microbiol. *5*, 1330–1339. https://doi.org/10.1038/s41564-020-0769-y.

21. Yu, J., Liang, C., and Liu, S.L. (2017). Interferon-inducible LY6E protein promotes HIV-1 infection. J. Biol. Chem. *292*, 4674–4685.

22. Yu, J., Liang, C., and Liu, S.L. (2019). CD4-Dependent modulation of HIV-1 entry by

LY6E. J. Virol. *93*, e01866-18. https://doi.org/10.1128/jvi.01866-18.

23. Giridharan, S., and Srinivasan, M. (2018). Mechanisms of NF-κB p65 and strategies for therapeutic manipulation. J. Inflamm. Res. *11*, 407–419. https://doi.org/10.2147/jir.S140188.

24. Kawasaki, T., and Kawai, T. (2014). Toll-like receptor signaling pathways. Front. Immunol. *5*, 461. https://doi.org/10.3389/fimmu.2014.00461.

25. Rajalingam, K., Wunder, C., Brinkmann, V., Churin, Y., Hekman, M., Sievers, C., Rapp, U.R., and Rudel, T. (2005). Prohibitin is required for Ras-induced Raf-MEK-ERK activation and epithelial cell migration. Nat. Cell Biol. *7*, 837–843. https://doi.org/10.1038/ncb1283.

26. Wintachai, P., Wikan, N., Kuadkitkan, A., Jaimipuk, T., Ubol, S., Pulmanausahakul, R., Auewarakul, P., Kasinrerk, W., Weng, W.Y., Panyasrivanit, M., et al. (2012). Identification of prohibitin as a Chikungunya virus receptor protein. J. Med. Virol. *84*, 1757–1770. https://doi.org/10.1002/jmv.23403.

27. Ma, W., Xu, Z., Wang, Y., Li, W., Wei, Z., Chen, T., Mou, T., Cheng, M., Luo, J., Luo, T., et al. (2018). A positive feedback loop of SLP2 activates MAPK signaling pathway to promote gastric cancer progression. Theranostics *8*, 5744–5757. https://doi.org/10.7150/thno.28898.

28. Wang, H., Zhou, Y., Oyang, L., Han, Y., Xia, L., Lin, J., Tang, Y., Su, M., Tan, S., Tian, Y., et al. (2019). LPLUNC1 stabilises PHB1 by counteracting TRIM21-mediated ubiquitination to inhibit NF-κB activity in nasopharyngeal carcinoma. Oncogene *38*, 5062–5075. https://doi.org/10.1038/s41388-019-0778-6.

29. Fitzgerald, K.A., and Kagan, J.C. (2020). Toll-like receptors and the control of immunity. Cell *180*, 1044–1066. https://doi.org/10.1016/j.cell.2020.02.041.

30. Häcker, H., Redecke, V., Blagoev, B., Kratchmarova, I., Hsu, L.C., Wang, G.G., Kamps, M.P., Raz, E., Wagner, H., Häcker, G., et al. (2006). Specificity in Toll-like receptor signalling through distinct effector functions of TRAF3 and TRAF6. Nature *439*, 204–207. https://doi.org/10.1038/nature04369.

31. Perkins, D.J., Richard, K., Hansen, A.-M., Lai, W., Nallar, S., Koller, B., and Vogel, S.N. (2018). Autocrine–paracrine prostaglandin E2 signaling restricts TLR4 internalization and TRIF signaling. Nat. Immunol. *19*, 1309–1318. https://doi.org/10.1038/s41590-018-0243-7.

32. Prodromou, C. (2016). Mechanisms of Hsp90 regulation. Biochem. J. *473*, 2439–2452. https://doi.org/10.1042/bcj20160005.

33. Morán Luengo, T., Mayer, M.P., and Rüdiger, S.G.D. (2019). The Hsp70-Hsp90 chaperone cascade in protein folding. Trends Cell Biol. *29*, 164–177. https://doi.org/10.1016/j.tcb.2018.10.004.

34. Hernando-Rodríguez, B., and Artal-Sanz, M. (2018). Mitochondrial quality control mechanisms and the PHB (prohibitin) complex. Cells *7*. https://doi.org/10.3390/cells7120238.

35. Buehler, U., Schulenburg, K., Yurugi, H., Šolman, M., Abankwa, D., Ulges, A., Tenzer, S., Bopp, T., Thiede, B., Zipp, F., and Rajalingam, K. (2018). Targeting prohibitins at the cell surface prevents Th17-mediated autoimmunity. The EMBO journal *37*, e99429. https://doi.org/10.15252/embj.201899429.

36. Hirata, T., Mishra, S.K., Nakamura, S., Saito, K., Motooka, D., Takada, Y., Kanzawa, N., Murakami, Y., Maeda, Y., Fujita, M., et al. (2018). Identification of a Golgi GPI-N-acetylgalactosamine transferase with tandem transmembrane regions in the catalytic domain. Nat. Commun. *9*, 405. https://doi.org/10.1038/s41467-017-02799-0.

37. Wang, Y., Liao, J., Yang, Y.J., Wang, Z., Qin, F., Zhu, S.M., Zheng, H., and Wang, Y.P. (2018). Effect of membrane-bound complement regulatory proteins on tumor cell sensitivity to complement-dependent cytolysis triggered by heterologous expression of the α-gal xenoantigen. Oncol. Lett. *15*, 9061–9068. https://doi.org/10.3892/ol.2018.8478.

STAR★METHODS

KEY RESOURCES TABLE

REAGENT or RESOURCE	SOURCE	IDENTIFIER
Antibodies		
HSP90AA1 Rabbit pAb	ABclonal	Cat# A12448; RRID: AB_2759291
HSP90AB1 Rabbit pAb	ABclonal	Cat# A1087; RRID: AB_2758283
EIF4A1 Rabbit pAb	ABclonal	Cat# A5294; RRID: AB_2766106
EEF1G Rabbit pAb	ABclonal	Cat# A2721; RRID: AB_2764572
LY6E Rabbit pAb	ABclonal	Cat# A10225; RRID: AB_2757749
CD14 Rabbit mAb	ABclonal	Cat# A19011; RRID: AB_2862503
Prohibitin Rabbit pAb	ABclonal	Cat# A0056; RRID: AB_2756921
SKP2 Rabbit pAb	ABclonal	Cat# A7728; AB_2772237
TRIM21/SS-A Rabbit pAb	ABclonal	Cat# A1957; RRID: AB_2763983
GAPDH Mouse mAb	ABclonal	Cat# AC002; RRID: AB_2736879
β-Actin Mouse mAb	ABclonal	Cat# AC004; RRID: AB_2737399
Monoclonal ANTI-FLAG® M2	Sigma	Cat# F1804; RRID: AB_262044
Mouse Anti-His mAB	ZSGB-BIO	Cat# TA-02; RRID: AB_2801388
goat anti-mouse IgG-HRP	ZSGB-BIO	Cat# ZB-2305; RRID: AB_2747415
goat anti-rabbit IgG-HRP	ZSGB-BIO	Cat# ZB-2301; RRID: AB_2747412
IκBα (L35A5) Mouse mAb	CST	Cat# 4814; RRID: AB_390781
Phospho-IκBα (Ser32/36) (5A5) Mouse mAb	CST	Cat# 9246; RRID: AB_2267145
NF-κB p65 (D14E12) XP® Rabbit mAb	CST	Cat# 8242; RRID: AB_10859369
Phospho-NF-κB p65 (Ser536) (93H1) Rabbit mAb	CST	Cat# 3033; RRID: AB_331284
Chemicals, peptides, and recombinant proteins		
Lipoplysaccharides from *Escherichia coli* O111:B4	Sigma	L3012
3×FLAG® Peptide	Sigma	F4799
Triton X-100	Sigma	X100
Direct-zol™ RNA MiniPrep	ZYMO	R2052
Experimental models: Cell lines		
HEK-293T cell	ATCC	N/A
THP-1 cell	ATCC	N/A
Oligonucleotides		
GAPDH forward primer: ACGGATTTGGTCGTATTGGG	This paper	N/A
GAPDH reverse primer: ATCTCGCTCCTGGAAGATGG	This paper	N/A
CD14 forward primer: GGAAGACTTATCGACCATGGAGC	This paper	N/A
CD14 reverse primer: CAGACACACACTGGAAGGCT	This paper	N/A
TNF-α forward primer:	This paper	N/A
TNF-α reverse primer:	This paper	N/A
IL-6 forward primer: GGCACTGGCAGAAAACAACC	This paper	N/A

(*Continued on next page*)

Continued

REAGENT or RESOURCE	SOURCE	IDENTIFIER
IL-6 reverse primer: GCAAGTCTCCTCATTGAATCC	This paper	N/A
IL-1β forward primer: AAACAGATGAAGTGCTCCTTCC	This paper	N/A
IL-1β reverse primer: AAGATGAAGGGAAAGAAGGTGC	This paper	N/A
IL-8 forward primer: GGCACAAACTTTCAGAGACAG	This paper	N/A
IL-8 reverse primer: ACACAGAGCTGCAGAAATCAGG	This paper	N/A
IFN-α forward primer: ACAGAGGACCATGCTGACTG	This paper	N/A
IFN-α reverse primer: TCAGGTTGCACAATTAGGCT	This paper	N/A
Software and algorithms		
FlowJo	BD Biosciences	Version 10
LEGENplex	BioLegend	Version 8.0
GraphPad PRISM	GraphPad Software	Version 8.2.1
Other		
Human Anti-Virus Response Panel (13-plex)	BioLegend	740390
Human Inflammatory Cytokin CBA Kit	BD Biosciences	551811
Mem-PERTM Plus Membrane Protein Extraction Kit	Thermo	89842
PI-PLC	Invitrogen	P6466
1×protease inhibitor cocktail	Thermo	78425
Pierce protein A/G agarose	Sigma	20422
anti-FLAG M2 affinity gel	Sigma	A2220

RESOURCE AVAILABILITY

Lead contact

Further information and requests for resources and reagents should be directed to and will be fulfilled by the lead contact, Jianqing Xu (xujianqing@fudan.edu.cn).

Materials availability

This study did not generate new unique reagents.

Data and code availability

- Original western blot images have been deposited at Mendeley Data: https://doi.org/10.17632/rpn25t3dsb.1 and are publicly available as of the date of publication.
- This paper dose not report original code.
- Any additional information required to reanalyze the data reported in this paper is available from the lead contact upon request.

EXPERIMENTAL MODEL AND SUBJECT DETAILS

Cell lines

The HEK-293T and THP-1 cell lines were purchased from American Type Culture Collection. The HEK-293T cells were maintained in Dulbecco's Modified Eagle Medium (DMEM; BI, Israel) supplemented with 10%

FBS (BI) and 1% penicillin and streptomycin (PS). The THP-1 cells were cultured in RPMI 1640 (BI) containing 15% FBS and 1% PS.

Plasmids

The lentiviral vectors encoding 3×FLAG-S-LY6E or 3×FLAG-LY6E were constructed by inserting the 3×FLAG-S-LY6E or 3×FLAG-LY6E sequence, which were generated by adding the corresponding tag sequence between the 23rd and 24th amino acid of LY6E sequence through overlapping PCR using pWPI-LY6E (the procedures to construct this plasmid was detailedly introduced in our previous study[12]) as the template, into pHAGE-CMV-IRES-zsGreen (Addgene plasmid #26532) between NheI and BamHI sites. pHAGE-PHB1 was obtained from Generay. To generate the lentiviral vector encoding a C-terminally 3×FLAG-tagged PHB1 (pHAGE-PHB1-3×FLAG), 3×FLAG was added to the end of PHB1 by PCR using pHAGE-PHB1 as the template and the resulting sequence was inserted into pHAGE-CMV-IRES-zsGreen as a NheI/BamHI fragment. PCMV-FLAG-CD14, encoding CD14 with a FLAG-tag inserted after the signal peptide, was purchased from SinoBiological (HG10073-NF). CD14 expressing plasmid was constructed by subcloning CD14 sequence into pWPI vector as a SpeI-NdeI fragment. Seven shRNA-expressing lentiviral vectors were used in the study: pLKO-LY6E-shRNA for LY6E targeting and pLKO-non-target-shRNA for non-targeting control were purchased from Sigma; pLKO-SKP2-shRNA for SKP2 targeting and pLKO-TRIM21-shRNA for TRIM2 targeting were constructed by Geneary (Shanghai, China) with AAGGTCTCTGGTGTTTGTAAG and AGTATCAGCCACGGATTGG as the targeting sequence, respectively; three PHB1-specific shRNAs were designed to target CCCAGAAATCACTGTGAAATT(sh1), GCTGCCGTCCATCACAACTGA (sh2), GAGTTCACAGAAGCGGTGGAA (sh3), and the corresponding lentiviral vectors were generated by subcloning the annealed oligonucleotides encoding shRNAs, which were synthesized by Geneary. Into TRC2-pLKO-puro using EcoRI and BshTI as the cloning sites.

METHOD DETAILS

Lentiviral transduction

For lentivirus production, 1×10^7 HEK-293T cells were plated in a 15 cm dish and 24 hrs later, transfected with a total of 15 μg of DNA mixture containing transfer plasmid, pSPAX2, and pVSV-G helper plasmid at 2:1:1 ratio. 48 hours post transfection, the supernatants were harvested, filtered through a 0.45 μm filter, and stored at -80°C as until use. For lentiviral transduction, lentivirus was added to target cells in the presence of polybrene (1 μg/mL) and after 6-8 hrs' incubation, the virus was replaced by fresh culture medium. When THP-1 cells were used as target cells, a 2 hrs' centrifugation at 1000×g was performed after adding the lentivirus.

RT-qPCR

RNA was extracted from 3×10^5 cells using Direct-zol™ RNA MiniPrep (ZYMO, R2052) according to the manufacturer's protocol. Reverse transcription of RNA into cDNA was performed using Reverse Transcription System (Promega # A3500). The resultant cDNAs were then subjected to quantitative PCR analyses conducted on a 7300 real-time PCR cycler (Applied Biosystems) by using gene-specific primers and GoTaq qPCR master mix (Promega, A6001).

LPS stimulation

For the assessments of early LPS-stimulated cellular response, 3×10^5 THP-1 cells per well were plated in a 48-well format and treated with 100 ng/mL of Lipopolysaccharides (LPS) derived from *Escherichia coli* O111:B4 (Sigma, L3012) for 0, 10, and 20 minutes. The cells were subjected to immunoblotting analysis to reveal the phosphorylation states of IκBα and NF-κB p65 subunit. For measuring the LPS-induced production of proinflammatory cytokine, 1.5×10^5 THP-1 cells per well were plated in a 96-well format using U-bottom plate and after stimulation with 100 ng/mL LPS for 6 hrs, the supernatants were collected for cytokine determinations using ELISA Set (BD Biosciences) or Human Anti-Virus Response Panel (13-plex) (Biolegend, 740390) following the manufacturers' instructions, and the cells for mRNA measurements using RT-qPCR.

PI-PLC treatment

Cells were harvested and washed with PBS, and subsequently resuspended in DMEM containing 1 U/mL PI-PLC (Invitrogen, P6466).[36,37] After incubated at 37°C for 2 hrs, cells were washed with PBS and collected for immunoblotting analyses.

Fractionation analyses

The separation of cytosolic and membrane fractions was performed using a Mem-PER™ Plus Membrane Protein Extraction Kit from Thermo Scientific (No.89842). The separation of detergent-resistant membrane (DRM) and non-DRM fractions followed a previously published procedure.[36] In brief, cells were collected, washed with ice cold PBS, and then resuspended in lysis buffer containing 50 mM Tris-HCl (pH 7.4), 150 mM NaCl, 1% Triton X-100, 5 mM EDTA, and 1×protease inhibitor cocktail (Thermo, 78425). After incubation at 4°C for 30 mins, the tubes were centrifuged at 21300×g for 20min at 4°C and supernatants were collected as Triton-soluble fraction (S). The precipitates were incubated with the second extraction buffer containing 50 mM Tris-HCl (pH 7.4), 150 mM NaCl, 60 mM Octyl-β-D-glucoside, 1 mM EDTA, and 1×protease inhibitor cocktail at 4°C for 30 mins prior to centrifugation under the condition the same as the first extraction, the resulting supernatants were collected as Triton-resistant fraction (R). The S and R samples were mixed with 4×SDS loading buffer (Takara, 631232) and boiled for 5 mins before subjecting to immunoblotting analyses.

Immunoblotting

The cells were lysed with 4×SDS loading buffer and boiled for 10 mins. The resultant protein samples were separated by SDS-PAGE electrophoresis and subsequently transfer to PVDF membranes (GE Healthcare). The membranes were blocked with 5% milk in the TBST buffer 1 hr at room temperature (RT), incubated overnight at 4°C with diluted primary antibodies, and subsequently exposed to diluted secondary antibodies at RT for 1 hr after extensive washing in TBST. The dilutions of antibodies were made in TBST+5% milk. The blots were rinsed extensively with TBST and then developed using ECL detection reagents (Amersham, RPN2232); the images were acquired by a LI-COR scanner and analyzed using Image Studio (LI-COR Biosciences). The following antibodies were used in this study: anti-LY6E (ABclonal, A10225) (1:1000), anti-HSP90AA1(ABclonal, A12448) (1:1000), anti-HSP90AB1 (ABclonal, A1087) (1:1000), anti-EIF4A1(ABclonal, A5294) (1:1000), anti-EEF1G (ABclonal, A2721) (1:1000), anti-CD14 (ABclonal, A19011) (1:1000), anti-PHB1 (ABclonal, A0056) (1:1000), anti-SKP2 (ABclonal, A7728) (1:1000), anti-TRIM21(ABclonal, A1957) (1:1000), anti-FLAG M2 (Sigma, F1804) (1:4000), anti-HIS (ZSGB-BIO, TA-02) (1:4000), anti-IκBα (CST, 4814S) (1:1000), anti-phospho-IκBα (CST, 9246S) (1:1000), anti-p65 (CST, 8242S) (1:1000), anti-phospho-p65 (CST,3033S) (1:1000), anti-β-actin (ABclonal, AC004) (1:5000), anti-GAPDH (ABclonal, AC002) (1:5000), goat anti-mouse IgG-HRP (ZSGB-BIO, ZB-2305) (1:5000), goat anti-rabbit IgG-HRP (ZSGB-BIO, ZB-2301) (1:5000).

Co-immunoprecipitations

Co-immunoprecipitations were performed with bait proteins with a single 1×or 3×FLAG or double 3×FLAG and S-tag. All the steps for co-immunoprecipitation were carried out on ice and with cold buffer. Cells stably or transiently expressing bait proteins were collected by 5-min centrifugation at 400×g at 4°C, rinsed twice with PBS, and resuspended in 0.8 mL of buffer A (10 mM Tris pH 7.3, 10 mM KCl, 1.5 mM $MgCl_2$, 10 mM β-Mercaptoethanol) supplemented with 1×protease and phosphatase inhibitor cocktail (Thermo, 78442) after rinsing once with buffer A. After incubation on ice for 10 mins, the cell suspensions were transferred to a 5 mL tissue homogenizer and 20 strokes were applied for cell disruption. After the removal of nuclei by centrifugation at 1000×g at 10 mins, the supernatants, corresponding to cytoplasmic extracts, were transferred to a new tube and mixed with equal volume of buffer B (50 mM Tris pH 7.3, 290 mM NaCl, 1.5 mM $MgCl_2$, 10% NP40). The resultant mixtures were incubated on ice for 20 mins and then cleared by centrifugation at 1000×g for 10 mins at 4°C. The supernatants were removed to a new tube, pre-cleaned via incubation with Pierce protein A/G agarose (Sigma, 20422) for 4 hrs at 4°C, and subsequently mixed with 40 μL of anti-FLAG M2 affinity gel (Sigma, A2220), followed by overnight incubation at 4°C. After extensive washing with cold wash buffer (50 mM Tris pH 7.3, 150 mM NaCl, 0.5% NP40), the immunoprecipitated proteins were eluted from the beads with 1 μg/mL of 3×FLAG peptide (Sigma, F4799). In the case of where a second S-tag purification was needed, the FLAG peptide eluates were subsequently incubated with 30 μL of S-protein Agarose (Millipore, 69704) at 4°C for 4 hrs. After extensive washing with wash buffer, the S-protein Agaroses were pelleted by centrifugation and the bound proteins were eluted by boiling in SDS buffer for 5 mins. The coimmunoprecipitation samples were used for immunoblotting analyses or visualized by silver staining for LC-MS/MS-based mass spectrometry analyses.

Ubiquitination assays

8 μg of pCMV-FLAG-CD14 or negative control plasmid was co-transfected with 8 μg of pcDNA3.0-His-ubquitin into different HEK-293T cell lines (1×10^7 cells per 15 cm dish). The transfected cells were cultured for an additional 48 hrs, and were then treated with MG132 (10 μM) for 12 hrs before lysis. Cell extract preparation and FLAG immunoprecipitation were performed following the same procedures as described above; the immuoprecipitaes, alongside the input lysates, were analyzed by immunoblotting with anti-His and anti-FLAG antibody. The presence of GADPH was simultaneously probed with GADPH-specific antibody for the demonstration of pulldown specificity.

Flow cytometry analyses

2×10^5 cells were collected and after wash with PBS containing 2% FBS, were subsequently stained with the CD14-APC (BD Biosciences) at room temperature for 20mins. The stained cells were acquired on a LSRFortessa flow cytometer (BD Biosciences) and the flow data was analyzed using FlowJo software.

QUANTIFICATION AND STATISTICAL ANALYSIS

Statistical analyses

Statistical analyses were performed in GraphPad Prism 8. Data are presented as means ± SEMs. Student's t test was used for nonpaired comparisons of two groups; two-way analysis of variance (ANOVA) was applied when more than two groups were compared. A p value of < 0.05 was considered to be statistically significant. All experiments reported in the paper were repeated three times.